UDK 666.112.2:615.281.9
Original scientific article/Izvirni znanstveni članek

ISSN 1580-2949
Mater. Tehnol.

PREPARATION AND ANTIBACTERIAL PROPERTIES OF CEFTAZIDIME-LOADED POLYCAPROLACTONE COATING/NANO-LITHIUM MAGNESIUM SILICATE-DOPED BIOACTIVE GLASS THREE-DIMENSIONAL SCAFFOLDS

PRIPRAVA IN ANTIBAKTERIJSKE LASTNOSTI POLIKAPROLAKTONSKE PREVLEKE POLNJENE S CEFTAZIDIMOM ZA TRIDIMENZIONALNA OGRODJA IZ BIOAKTIVNEGA STEKLA, DOPIRANEGA Z NANO-LITIJ-MAGNEZIJEVIM SILIKATOM

Jin Xie, Qijin Cao, Xiao Zheng*

Department of Ophthalmology, Pingyang Hospital affiliated with Wenzhou Medical University, Wenzhou 325400, Zhejiang Province, China

Prejem rokopisa – received: 2024-12-20; sprejem za objavo – accepted for publication: 2025-02-26

doi:10.17222/mit.2024.1358

We aimed to explore the preparation of three-dimensional scaffolds made from ceftazidime-loaded polycaprolactone-coated/nano-magnesium lithium silicate-doped bioactive glass (BG) and their antibacterial properties. Three-dimensional porous 45S5 BG and nano-magnesium lithium silicate, also known as laponite (Lap), were prepared using template replication combined with high-temperature sintering technology, so as to obtain BG-Lap scaffolds. Then the surface of BG-Lap scaffolds was coated with a mixture of polycaprolactone (PCL) and ceftazidime (CAZ) through dip coating, thus producing BG-Lap/PCL-CAZ composite scaffolds. The OD value increased significantly after 7 d compared with that after 4 d ($P < 0.05$). However, after 4 d and 7 d, this value was significantly higher in the control group than in the BG-Lap/PCL-CAZ group ($P < 0.05$). In the BG-Lap/PCL-CAZ group, significant increases in the cell survival rate were detected after 4 d and 7 d compared to 1 d, and it was significantly higher after 7 d than after 4 d. Compared with the BG-Lap/PCL-CAZ group, the control group exhibited a significantly raised cell survival rate after 4 d. The BG-Lap/PCL-CAZ composite scaffolds exhibit high porosity, which is conducive to cell growth and nutrient transport.

Keywords: antibacterial properties, bioactive glass, ceftazidime, magnesium lithium silicate, polycaprolactone, scaffold

Avtorji v tem članku opisujejo raziskavo izdelave in bakterioloških lastnosti tridimenzionalnega (3D) ogrodja iz nano-bioaktivnega silikatnega stekla dopiranega z Mg in Li ter prevlečenega s prevleko iz polikaproktalona napolnjenega z ceftadizimom. Porozno 3D bioaktivno steklo 45S5 in nano Mg-Li silikat (prav tako poznan kot laponit) sta bila pripravljena s kombinirano tehnologijo repliciranja na podlago in tehnologije visoko temperaturnega sintranja, tako da so izdelali bioaktivno laponitno (BG-Lap) ogrodje. Nato so to BG-Lap ogrodje s postopkom globokega potaplajanja prevlekli z mešanico polikaprolaktona (PCL) in ceftazidima (CAZ; antibiotik iz skupine cefalosporinov) in na ta način izdelali BG-Lap/PCL-CAZ kompozitno ogrodje. Vrednost za optično gostoto (OD; angl.: optical density) se je pomembno povečala na 7 d v primerjavi s 4 d ($P<0,05$), ter pri 4 d in 7 d sta bili ti dve vrednosti znatno višji v kontrolni skupini kot pri BG-Lap/PCL-CAZ skupini ($P<0,05$). Avtorji so opazili , da je v BG-Lap/PCL-CAZ skupini prišlo do pomembnega povečanja hitrosti preživetja celic 4 d in 7 d v nasprotju z 1 d ($P<0,05$) in znatno višje pri 7 d kot pri 4 d ($P<0,05$). V primerjavi z BG-Lap/PCL-CAZ skupino je kontrolna skupina pokazala pomembno povišanje hitrosti celičnega preživetja pri 4 d ($P<0,05$). Kompozitno ogrodje BG-Lap/PCL-CAZ je bolj porozno in je zato tudi bolj prevodno za rast celic in transport hranil.

Ključne besede: antibakterijske lastnosti, bioaktivno steklo, ceftazidim; magnezij-litijev silikat, polikaprolakton, ogrodje

1 INTRODUCTION

With the continuous development of medical technology, biomaterials have witnessed a more extensive application. Among these, bioactive glass (BG) has attracted widespread attention due to excellent biocompatibility, osteoconductivity, and bone-bonding ability. As a result, BG has been widely applied in bone defect repair, tooth regeneration and tissue engineering.[1–3] However, traditional BG scaffolds have deficiencies in antibacterial properties, which often render them inadequate in addressing the complex clinical needs of patients with infected bone defects.[4] Therefore, the development of BG scaffolds with antibacterial properties has become a focus of research.

Recent development in material science has focused on enhancing the antibacterial properties of BG scaffolds to overcome these limitations. Incorporating antimicrobial agents into BG scaffolds has become a promising approach to improve their efficacy. One such agent is ceftazidime (CAZ), a third-generation cephalosporin antibiotic known for its broad-spectrum antibacterial activity, especially against gram-negative bacteria. CAZ is commonly used in clinical practice to treat a variety of bacterial infections, and its incorporation into scaffolds

*Corresponding author's e-mail:
zhengxiaophwmu@wl-asia.com (Xiao Zheng)

may combat bacterial infections at the site of implantation, thus improving the healing outcomes.[5]

In addition, polycaprolactone (PCL) is a biodegradable polymer material with desirable biocompatibility and plasticity. Its slow degradation rate and ease of processing make it an ideal candidate for use in drug-controlled release systems and tissue engineering applications.[6] By incorporating PCL into BG scaffolds, a sustained release of therapeutic agents such as CAZ can be achieved, contributing to both antibacterial effects and enhanced tissue regeneration. Moreover, the addition of inorganic nanomaterials such as nano-magnesium lithium silicate [laponite (Lap)] has great potential in improving the mechanical properties and bioactivity of scaffolds. It has a unique layered structure and excellent dispersion properties, which can enhance the overall mechanical strength and stability of scaffolds.[7] By introducing Lap into BG scaffolds, it is possible to improve their mechanical support and bioactivity, further boosting their suitability for bone defect repair and tissue engineering.

In this study, therefore, CAZ, PCL and Lap were combined with BG to prepare novel BG-Lap/PCL-CAZ composite scaffolds, and their antibacterial properties and cell survival rate were evaluated. By optimizing the preparation process and parameters, we expected to produce BG scaffolds with excellent antibacterial properties and biocompatibility, thereby providing a new option for bone defect repair and anti-infective treatment in clinical practice.

2 EXPERIMENTAL PART

2.1 Main reagents and apparatuses

45S5 BG powders were purchased from Suzhou Ding'an Technology Co., Ltd. (China). Lap powders were obtained from Beijing Yiwei Specialized Technology Development Co., Ltd. (China). PCL was bought from Sigma (USA). Polyurethane film was provided by Eurofoam GmbH (Germany). An S-3000N scanning electron microscope (SEM) was purchased from Hitachi (Japan). A Q150T pumped coater was obtained from Quorum (UK).

2.2 Preparation and physicochemical characterization of BG-Lap/PCL-CAZ composite scaffolds

A total of 0.4 g PCL was weighed and added into 10 mL of dimethyl carbonate. After stirring and dissolving at 60 °C, it was cooled to room temperature. Then 45S5 BG powders and Lap powders were added to the solution and stirred evenly to obtain a mixed slurry. The pre-prepared (10 × 10 × 10) mm polyurethane film was soaked in the slurry, and then the excess slurry was squeezed out and dried in a 60 °C oven overnight to obtain a BG-Lap embryo. The aforementioned steps were repeated twice. Finally, BG-Lap scaffolds were obtained by high-temperature sintering.

After the PCL-containing dimethyl carbonate solution was prepared, a certain amount of CAZ was added to obtain a PCL-CAZ solution. Then the BG-Lap scaffolds were soaked in the PCL-CAZ solution for 10 s, removed, and dried to obtain BG-Lap/PCL-CAZ composite scaffolds. The drug release curve and antibacterial experiments were utilized to optimize the conditions.

2.3 SEM method

The scaffolds were fixed onto a copper plate with conductive glue. Then the coater was utilized to apply a layer of gold on the surface of the scaffolds to increase the conductivity. The sample morphology was observed and photographed using SEM at an accelerating voltage of 10 kV.

2.4 Systematic study of the porosity, micromorphology, pore size, mechanical properties and drug release curve of BG-Lap/PCL-CAZ composite scaffolds

The porosity of BG-Lap scaffolds [$P = (1–W/V{\cdot}\rho\ \rho) \times 100\ \%$] and ρ [$\rho = ((40\% \times \rho_{BG} + n\ \% \times \rho\rho_{Lap}) / 40\ \% + n\ \%$] were calculated. Here, P is the porosity of scaffolds, W represents the weight of scaffolds, and V is the volume of scaffolds, which is calculated by measuring the length, width and height of the scaffolds with a Vernier caliper; ρ_{BG} stands for the density of 45S5 BG, set as 2.7 g/cm^3; ρ_{Lap} refers to the density of Lap, being 2.53 g/cm^3; and n denotes the content of Lap. As for the measurement of porosity, 7 samples were selected and the average value was taken.

2.5 Cytotoxicity test of BG-Lap/PCL-CAZ composite scaffolds

MC-3T3 cells were inoculated at 1 × 10^5/well into 24-well plates containing 45S5 BG, BG-Lap, and BG-Lap/PCL-CAZ composite scaffolds, with 45S5 BG scaffolds as the control group. The cells were cultured for 24 h and rinsed 2–3 times with a PBS solution 48 h later. Next, a culture medium containing a 10 % CCK-8 solution was added to each well for 1 h of incubation in a constant-temperature (37 °C) incubator with 5-% CO_2. Afterwards, 100 µL of supernatant was transferred to a 96-well plate, and the optical density (OD) was measured at 450 nm using an enzyme reader. The cell survival and proliferation rates were calculated.

The following calculation formulas were used: cell survival rate = single measurement of OD value / total measurement mean; cell proliferation rate = single measurement of OD value / total measurement mean on the first day. The OD value, cell survival rate and cell proliferation rate were observed after (1, 4 and 7) d of the experiment.

2.6 Statistical analysis

Statistical software SPSS 27.0 was employed for data processing. Count data were expressed as [n (%)] and subjected to the χ^2 test. Measurement data that conformed to normal distribution were described in the format of ($\bar{x} \pm s$). Repeated measures analysis of variance was conducted for the results of the antibacterial test on the BG-Lap/PCL-CAZ composite scaffolds after (1, 4, and 7) d, involving the OD value, cell survival rate, and cell proliferation rate. Post hoc comparisons were performed using the least significant difference *t* test. $P < 0.05$ denoted a difference of statistical significance.

3 RESULTS

3.1 Characterization of BG-Lap scaffolds using SEM

The large pore size of scaffolds is not only conducive to cell migration but also favourable for the formation of blood vessels in the scaffolds. **Figure 1** shows SEM images of the three scaffolds (45S5 BG, BG-1Lap, and BG-3Lap).

As shown in **Figures 1a–c**, all the three scaffolds have a good through-porous structure. The pore size of the BG-3LAP scaffold was smaller than those of the 45S5 BG and BG-1LAP scaffolds, ranging from 100 μm to 500 μm, which may be conducive to the growth of cells and the formation of blood vessels in the scaffold.

In addition, it is indicated in **Figures 1d–f** that the scaffolds have a granular surface with a nanoscale microporous structure. The presence of a large number of micropores was conducive to increasing the specific surface area of the scaffolds.

3.2 In vitro hydroxyapatite formation

According to the results of the *in-vitro* hydroxyapatite formation of BG-Lap scaffolds (**Figure 2**), when the scaffolds were immersed in a simulated body fluid for 1 day, apatite-like crystals were formed on the surfaces of all scaffolds. Despite different crystal formation methods, crystals were formed in a larger number and with a smaller size in the BG-3Lap scaffold than in the 45S5 BG scaffold. On the 4th day (**Figures 2d**, **2f**), however, a typical cauliflower-like hydroxyapatite formation was observed in all scaffolds. Results of the energy spectrum analysis showed that the ratio of calcium to phosphorus was about 1.67:1, similar to that of hydroxyapatite in the human body, indicating that the addition of Lap does not interfere with the formation of apatite. After implantation in the body, the BG-3Lap scaffold is comparable to the 45S5 BG scaffold in terms of the bone-bonding ability.

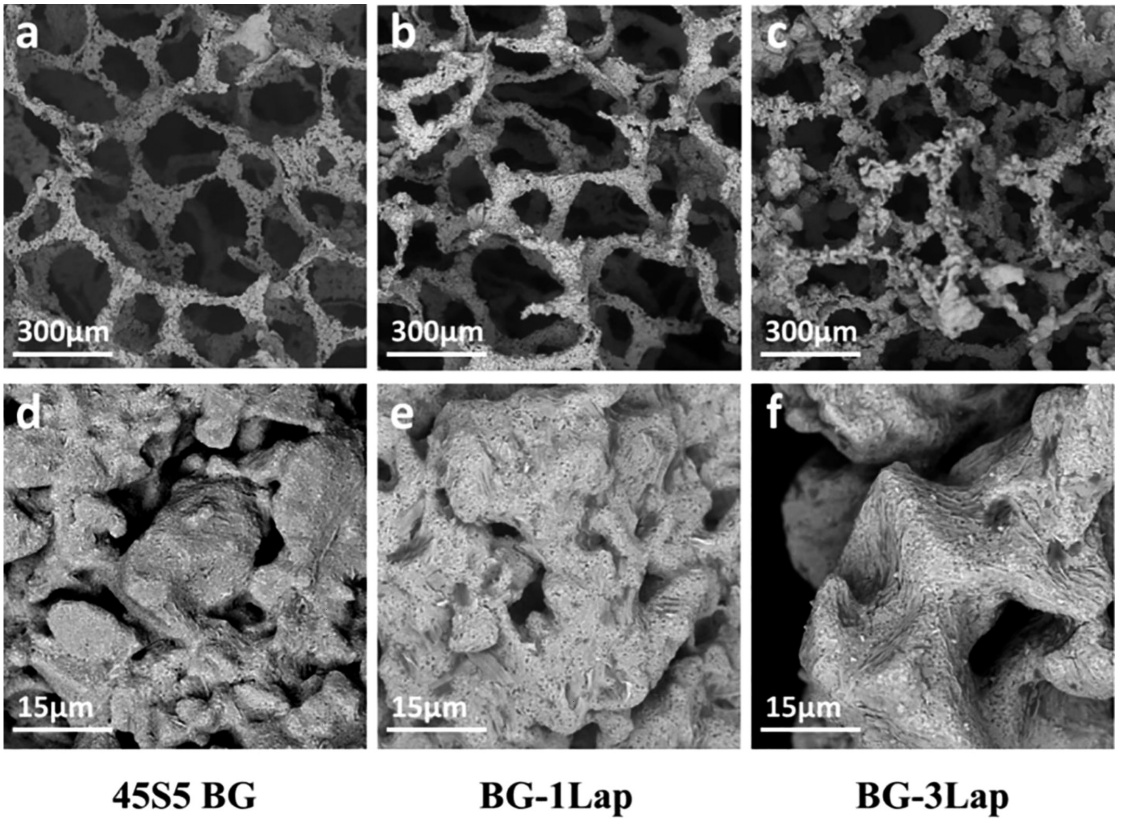

Figure 1: SEM images of 45S5 BG (a, d), BG-1Lap (b, e), and BG-3Lap (c, f) scaffolds. BG: bioactive glass; Lap: laponite; SEM: scanning electron microscopy

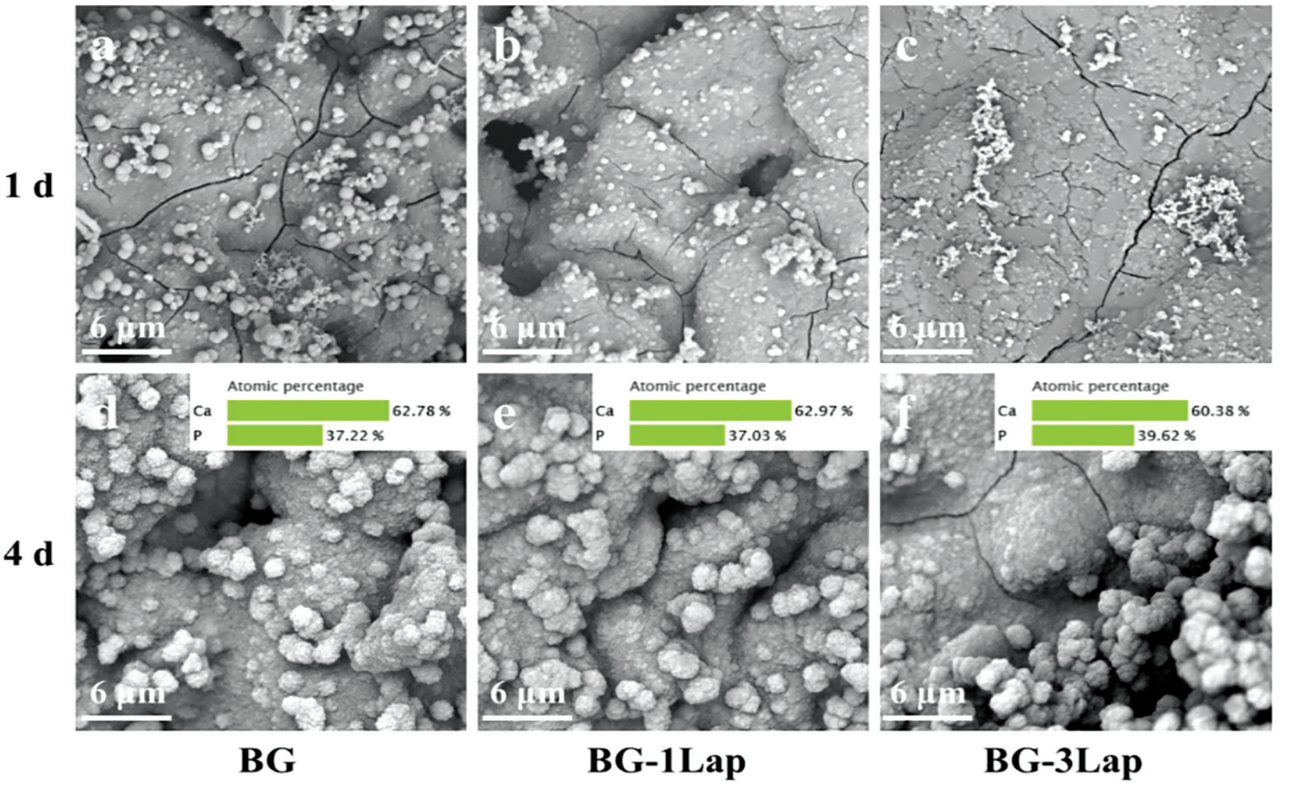

Figure 2: SEM images and energy spectrum analysis of 45S5 BG (a, d), BG-1Lap (b, e) and BG-3Lap (c, f) scaffolds immersed in simulated body fluid for 1 and 4 d. BG: bioactive glass; Lap: laponite; SEM: scanning electron microscopy

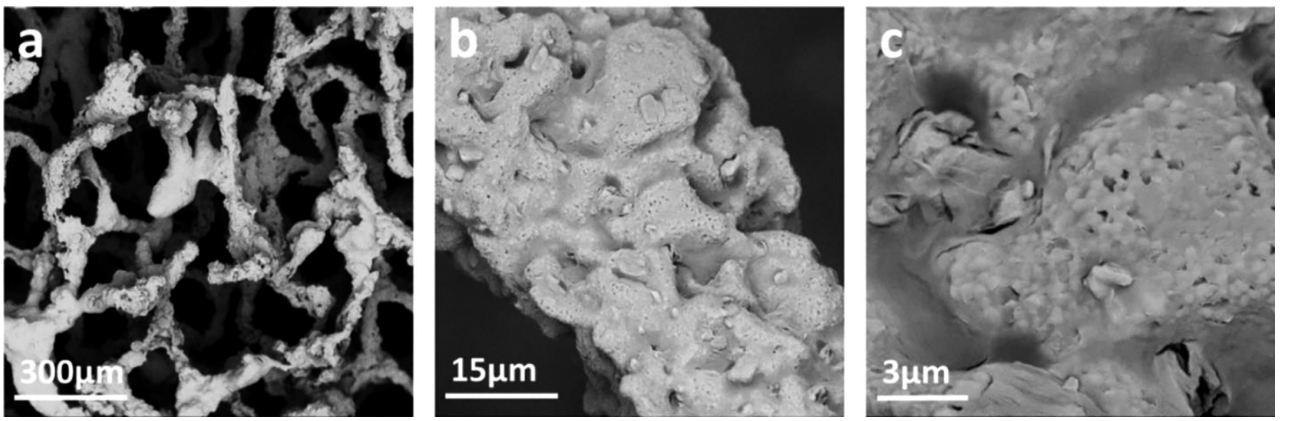

Figure 3: SEM images of BG-3Lap/PCL-CAZ composite scaffolds. BG: bioactive glass; CAZ: ceftazidime; Lap: laponite; PCL: polycaprolactone; SEM: scanning electron microscopy

Table 1: BG-Lap/PCL scaffold data

Data	No. 1	No. 2	No. 3	No. 4	No. 5	No. 6	No. 7
Weight (mg)	19.80	16.50	18.00	15.20	18.40	17.50	17.20
Side length (mm)	5.40	5.50	5.60	4.48	5.50	5.40	5.50
	5.70	4.40	5.80	5.56	5.55	5.19	5.40
	4.90	5.40	4.65	5.42	4.30	4.90	5.28
Porosity	95.14 %	95.32 %	95.59 %	95.83 %	94.81 %	95.28 %	95.94 %
Porosity ($\bar{x} \pm s$)	95.41 ± 0.40 %						

BG: bioactive glass; Lap: laponite; PCL: polycaprolactone

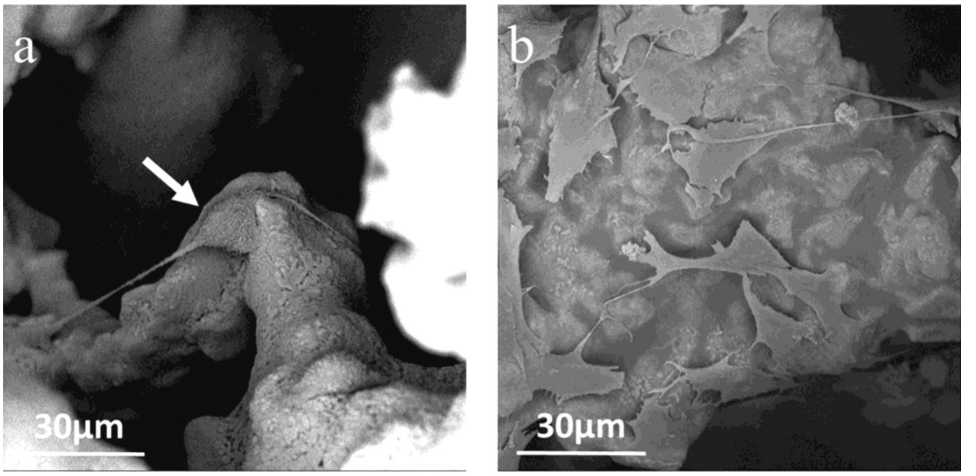

Figure 4: Results of cytotoxicity test of BG-Lap/PCL-CAZ composite scaffolds. BG: bioactive glass; CAZ: ceftazidime; Lap: laponite; PCL: polycaprolactone

3.3 SEM results of BG-Lap/PCL-CAZ composite scaffolds

After PCL coating on the surface, the BG-Lap scaffolds not only maintained the large porous structure, but also acquired a microporous structure allowing for the application and penetration of PCL, which was conducive to delaying the release of CAZ (**Figure 3**).

The weight and side length of the BG-Lap/PCL-CAZ composite scaffolds were measured seven times, and the porosity was calculated based on the measured porosity. It was found that the average porosity of the BG-Lap/PCL-CAZ composite scaffolds was (95.41 ± 0.40 %). Details are presented in **Table 1**.

3.4 Cytotoxicity test of BG-Lap/PCL-CAZ composite scaffolds

The cell morphology on the scaffold surface can directly reflect the cytotoxicity of the material. As shown in **Figure 4a**, after 1 day of culture, the cells adhered well to the surface of BG-3Lap/PCL-CAZ composite scaffolds; the cells were stretched, and pseudopodia were extended, suggesting that the cells grew in good condition. After 4 days of culture, as shown in **Figure 4b**, the number of cells was increased significantly; the cells became polygonal and tended to connect into sheets. The above results demonstrate that the cells can grow and proliferate well in the scaffolds, and that the scaffolds exhibit favourable cell compatibility.

As revealed by repeated measures ANOVA, there were statistically significant differences in the OD value and cell proliferation rate between the control group and the BG-Lap/PCL-CAZ group in terms of time point factor and group factor ($P < 0.05$). The difference in the cell survival rate was statistically significant, concerning the time point factor, time point interaction factor, and group factor. It was found through a post hoc LSD-*t* test that

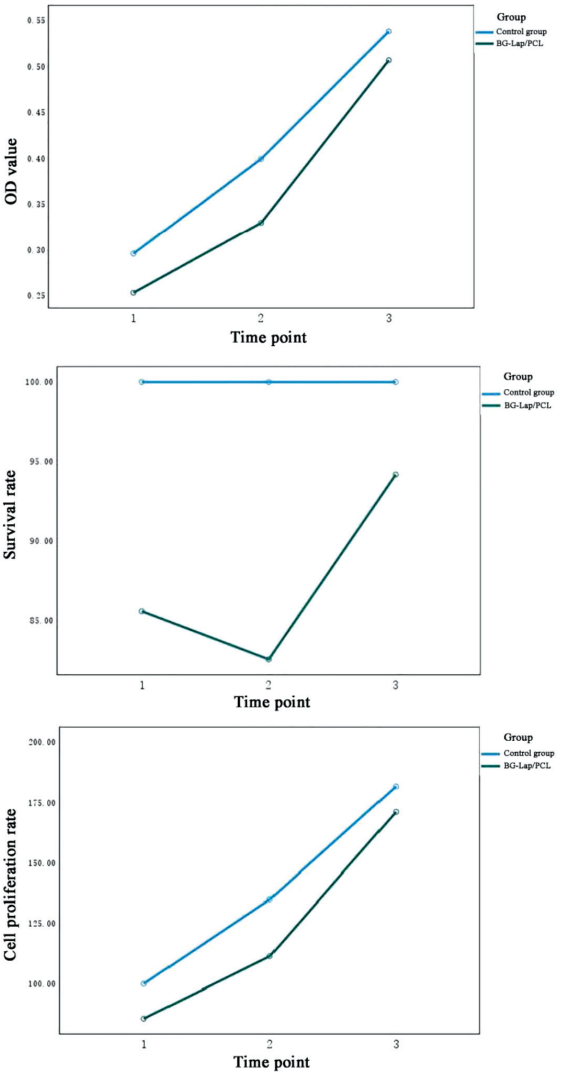

Figure 5: Time point profiles of OD value, cell survival rate and cell proliferation rate of BG-Lap/PCL-CAZ composite scaffolds obtained with cytotoxicity test. BG: bioactive glass; CAZ: ceftazidime; Lap: laponite; OD: optical density; PCL: polycaprolactone

Table 2: Cytotoxicity results for the BG-Lap/PCL-CZA scaffold

Indicator	Group (*n*)	1 d	4 d	7 d
Optical density	Control group (6)	$0.30\pm0.01^{\Delta}$	$0.40\pm0.01^{a\Delta}$	$0.54\pm0.02^{a\Delta}$
	BG-Lap/PCL (6)	0.25±0.01	0.33 ± 0.01^{a}	0.51 ± 0.04^{ab}
	F value	$F_{\text{time point}} = 722.581$	$F_{\text{Interaction}} = 0.378$	$F_{\text{Group}} = 41.976$
	P value	$P_{\text{time point}} < 0.001$	$P_{\text{Interaction}} = 0.553$	$P_{\text{Group}} < 0.001$
Survival rate	Control group (6)	$100.00\pm1.74^{\Delta}$	$100.00\pm2.98^{\Delta}$	100.00±4.63
	BG-Lap/PCL (6)	85.59±2.62	82.56 ± 3.72^{a}	94.18 ± 7.03^{ab}
	F value	$F_{\text{time point}} = 5.968$	$F_{\text{Interaction}} = 5.968$	$F_{\text{Group}} = 68.831$
	P value	$P_{\text{time point}} = 0.035$	$P_{\text{Interaction}} = 0.035$	$P_{\text{Group}} < 0.001$
Proliferation rate	Control group (6)	$100.00\pm1.74^{\Delta}$	$134.97\pm4.02^{a\Delta}$	181.81 ± 8.42^{ab}
	BG-Lap/PCL (6)	85.59±2.62	111.43 ± 5.03^{a}	171.23 ± 12.78^{ab}
	F value	$F_{\text{time point}} = 724.801$	$F_{\text{Interaction}} = 0.379$	$F_{\text{Group}} = 41.494$
	P value	$P_{\text{time point}} < 0.001$	$P_{\text{Interaction}} = 0.552$	$P_{\text{Group}} < 0.001$

the OD value and cell proliferation rate of both groups were significantly higher after 7 d and 4 d than after 1 d. Moreover, the OD value was increased significantly after 7 d compared with that after 4 d, and the control group exhibited a significantly higher OD value than the BG-Lap/PCL-CAZ group after 4 d and 7 d. In the BG-Lap/PCL-CAZ group, significant increases in the cell survival rate were detected after 4 d and 7 d compared to that after 1 d, and it was significantly higher after 7 d than after 4 d. Additionally, compared with the BG-Lap/PCL-CAZ group, the control group exhibited a significantly increased cell survival rate after 4 d. Details are exhibited in **Table 2** and **Figure 5**.

4 DISCUSSION

In this study, the BG-Lap/PCL-CAZ composite scaffolds had an average porosity of (95.41 ± 0.40 %), implying that the scaffolds have a good porous structure. High porosity not only facilitates cell penetration and growth, but also promotes vascularization and improves tissue regeneration.[8,9] Therefore, the BG-Lap/PCL-CAZ composite scaffolds have potential application in bone defect repair. Furthermore, high porosity is one of the important characteristics of tissue engineering scaffolds, with direct impacts on cell penetration, growth and differentiation. Herein, the average porosity of the BG-Lap/PCL-CAZ composite scaffolds was as high as (95.41 ± 0.40 %), providing ample space for cell growth. High porosity is not only conducive to cell migration and proliferation, but also favourable for the formation of blood vessels, thereby accelerating tissue regeneration and repair.[10,11] The OD value and cell proliferation rate of the control group were significantly different from those in the BG-Lap/PCL-CAZ group regarding the time point factor and group factor ($P < 0.05$). This suggests that the BG-Lap/PCL-CAZ composite scaffolds outperform the control scaffold in terms of antibacterial performance. Furthermore, the OD value and cell proliferation rate of the BG-Lap/PCL-CAZ composite scaffolds rose significantly after 7 d and 4 d in comparison to those after 1 d, and there was an increase after 7 d compared with the values after 4 d. These results suggest that the antibacterial properties of the scaffolds gradually increased over time and peaked after 7 d.

In addition, the OD value and cell proliferation rate of the control group were significantly higher than those of the BG-Lap/PCL-CAZ group after 4 and 7 d, further confirming the excellent antibacterial properties of the BG-Lap/PCL-CAZ composite scaffolds. Based on the analysis of the cell survival rate, the BG-Lap/PCL-CAZ group exhibited statistically significant differences in time point factors, time point interaction factors, and group factors, implying that the cell survival rate of the scaffolds is affected by multiple factors, but the BG-Lap/PCL-CAZ composite scaffolds have prominent advantages in all these factors. The cell survival rate was elevated in the BG-Lap/PCL-CAZ group after 4 and 7 d compared to that after 1 d, as well as the value after 7 d was higher than that after 4 d. This indicates that the cell survival rate of the scaffolds increased over time and reached the highest level after 7 days. However, the control group had a significantly higher cell survival rate than the BG-Lap/PCL-CAZ group after 4 d. This may be attributed to the fact that the control group had a higher cell survival rate in the early stage, which later gradually declined due to a lack of effective antibacterial properties.

Being a nanomaterial with excellent antibacterial properties, CAZ can effectively inhibit the growth and reproduction of bacteria. Its antibacterial mechanism may be related to the nano-effect and surface charge of CAZ, which can destroy the cell membrane structure of bacteria and cause bacterial death.[12,13] Besides, the broad-spectrum antibiotic CAZ has a strong antibacterial effect. After loading CAZ onto the scaffold surface with PCL coating, the drug can be slowly released, thereby continuously inhibiting the growth of bacteria. Such a drug release method not only improves the utilization rate of CAZ, but also reduces its side effects. PCL, a polymer material with good biocompatibility, can be prepared into a protective film to prevent direct contact between bacteria and scaffolds.[14,15] At the same time, the PCL coating can regulate the drug release rate, so that

the drug forms an effective antibacterial barrier inside and around the scaffolds.[16,17] The BG-Lap/PCL-CAZ group presented a remarkable increase in the survival rate after 4 d and 7 d compared with that after 1 day. This may be attributed to the fact that the porous structure and antibacterial properties of the scaffolds provide a good growth environment for cells.[18,19]

With extended time, the cells gradually proliferated inside the scaffolds to form a stable cell community. After 4 d, however, the cell survival rate increased distinctly in the control group compared to that in the BG-Lap/PCL-CAZ group, which was probably due to the higher cell survival rate in the control group in the initial stage. However, the cell survival rate in the control group decreased gradually over time because of the lack of effective antibacterial properties. On the contrary, the BG-Lap/PCL-CAZ composite scaffolds were able to continuously inhibit the growth of bacteria owing to their excellent antibacterial properties, thereby protecting cells from bacteria and improving their survival.[20,21]

Nevertheless, this study still has some limitations. For example, only a preliminary evaluation of the antibacterial properties of the BG-Lap/PCL-CAZ composite scaffolds was conducted, and no comprehensive study on their biocompatibility, bone-bonding ability and mechanical properties was carried out. In addition, regardless of the representative indicators such as OD, cell proliferation rate, and cell survival rate, the biological properties of the scaffolds are not fully presented. In the future, it is necessary to evaluate the biocompatibility of BG-Lap/PCL-CAZ composite scaffolds through animal experiments and cell culture methods to provide strong support for clinical applications. In the past, methods such as histological staining and mechanical testing were employed to explore the ability of BG-Lap/PCL-CAZ composite scaffolds to bind to bone tissues, aiming to render a theoretical basis for their application in bone defect repair. The mechanical properties of the scaffolds were optimized by adjusting the preparation process and material composition, so as to make them more compliant with the demands of clinical application. However, long-term follow-up observation of BG-Lap/PCL-CAZ composite scaffolds should be carried out to evaluate their long-term antibacterial effects and biocompatibility, thus rendering a reliable basis for clinical application.

Despite the above limitations, the present study introduces a novel BG-Lap/PCL-CAZ composite scaffold that combines high porosity (95.41 ± 0.40 %) with sustained antibacterial properties. This dual functionality is significant because it not only facilitates cell penetration, migration, and growth, promoting vascularization and tissue regeneration, but also creates a prolonged antibacterial barrier through a controlled release of CAZ through the PCL coating. To the best of our knowledge, this is one of the first studies to integrate CAZ in such a manner with BG-Lap/PCL scaffolds, providing a promising strategy for the repair of bone defects.

5 CONCLUSIONS

In conclusion, we successfully prepared three-dimensional BG-Lap/PCL-CAZ scaffolds by doping BG with CAZ-loaded PCL coating/nano-magnesium lithium silicate, and tested their antibacterial properties. The composite scaffolds exhibited an excellent porous structure and antibacterial properties, which can significantly improve the survival and proliferation rates of cells. Future studies will further optimize the mechanical properties, biocompatibility and bone-bonding ability of the scaffolds to provide strong support for their application in bone defect repair.

Acknowledgment

None.

Conflicts of interest

There are no conflicts of interest.

5 REFERENCES

[1] E. Kheradmand, A. Daneshkazemi, A. Davari, M. Kave, S. Ghanbarnejad, Effect of hydrogen peroxide and its combination with nano-hydroxyapatite or nano-bioactive glass on the enamel demineralization and tooth color: An in vitro study, Dent. Res. J., 25 (**2023**) 5, 85, PMID: 37674573

[2] R. Wu, L. Huang, Q. Xia, Z. Liu, Y. Huang, Y. Jiang, J. Wang, H. Ding, C. Zhu, Y. Song, L. Liu, L. Zhang, G. Feng, Injectable mesoporous bioactive glass/sodium alginate hydrogel loaded with melatonin for intervertebral disc regeneration, Mater. Today Bio, 17 (**2023**) 3, 100731, doi:10.1016/j.mtbio.2023.100731

[3] Z. Xu, X. Qi, M. Bao, T. Zhou, J. Shi, Z. Xu, M. Zhou, A. R. Boccaccini, K. Zheng, X. Jiang, Biomineralization inspired 3D printed bioactive glass nanocomposite scaffolds orchestrate diabetic bone regeneration by remodeling micromilieu, Bioact. Mater., 8 (**2023**) 25, 239–255, doi:10.1016/j.bioactmat.2023.01.024

[4] K. Elakkiya, C. Ashok Raja, S. Balakumar, Devitrite (Na2Ca3Si6O16) phase dominated nanostructured 45S5 bioactive glass: exploring its structural and biological properties, Biomed. Mater., 19 (**2024**) 2, 85–94, doi:10.1088/1748-605X/ad2708

[5] C. Jiang, G. Zhu, Q. Liu, Current application and future perspectives of antimicrobial degradable bone substitutes for chronic osteomyelitis, Front. Bioeng. Biotech., 12 (**2024**), 1375266, doi:10.3389/fbioe.2024.1375266

[6] H. Wu, X. Wei, X. Liu, H. Dong, Z. Tang, N. Wang, S. Bao, Z. Wu, L. Shi, X. Zheng, X. Li, Z. Guo, Dynamic degradation patterns of porous polycaprolactone/β-tricalcium phosphate composites orchestrate macrophage responses and immunoregulatory bone regeneration, Bioact. Mater., 6 (**2022**) 21, 595–611, doi:10.1016/j.bioactmat.2022.07.032

[7] K. M. Marshall, J. S. McLaren, J. S. Wojciechowski, S. J. P. Callens, C. Echalier, J. M. Kanczler, F. R. A. J. Rose, M. M. Stevens, J. I. Dawson, R. O. C. Oreffo, Bioactive coatings on 3D printed scaffolds for bone regeneration: Use of Laponite® to deliver BMP-2 in an ovine femoral condyle defect model, Biomater. Adv., 164 (**2024**), 213959, doi:10.1016/j.bioadv.2024.213959

[8] S. Wang, D. Xia, W. Dou, A. Chen, S. Xu, Bioactive Porous Composite Implant Guides Mesenchymal Stem Cell Differentiation and Migration to Accelerate Bone Reconstruction, Int. J. Nanomedicine, 19 (**2023**), 12111–12127, doi:10.2147/IJN.S479893

[9] W. J. Lee, K. Cho, D. Lee, S. Lee, H. Jeon, A. Y. Kim, G. W. Kim, Enhanced osteogenic potential of spider silk fibroin-based composite scaffolds incorporating carboxymethyl cellulose for bone tissue engineering, Biomater. Biosyst., 16 (**2024**), 100103, doi:10.1016/j.bbiosy.2024.100103

[10] M. Kazemi, H. Esmaeili, M. Khandaei Dastjerdi, F. Amiri, M. Mehdikhani, M. Rafienia, The impact of 45S5 bioglass vs. β-TCP nanoparticles ratio on rheological behavior of formulated printing inks and 3D printed polycaprolactone-based scaffolds final properties, Heliyon, 10 (**2024**) 22, e39219, doi:10.1016/j.heliyon.2024.e39219

[11] M. Vazifehdoust, A. Shalizar-Jalali, M. R. Nourani, M. R. Moosazadeh Moghaddam, M. Yazdanian, Improvement of osteogenesis and antibacterial properties of a bioactive glass/gelatin-based scaffold using zoledronic acid and CM11 peptide, Vet. Res. Forum, 15 (**2024**) 9, 487–498, doi:10.30466/vrf.2024.2020333.4136

[12] Y. C. Chou, Y. H. Hsu, D. Lee, J. W. Yang, Y. H. Yu, E. C. Chan, S. J. Liu, Novel Bioresorbable Drug-Eluting Mesh Scaffold for Therapy of Muscle Injury, ACS Biomater. Sci. Eng., 10 (**2024**) 4, 2595–2606, doi:10.1021/acsbiomaterials.3c01669

[13] S. Nezamoleslami, A. Fattahi, H. Nemati, F. Bagrezaie, Z. Pourmanouchehri, S. H. Kiaie, Electrospun sandwich-structured of polycaprolactone/gelatin-based nanofibers with controlled release of ceftazidime for wound dressing, Int. J. Biol. Macromol., 236 (**2023**), 123819, doi:10.1016/j.ijbiomac.2023.123819

[14] W. Akram, R. Zahid, R. M. Usama, S. A. AlQahtani, M. Dahshan, M. A. Basit, M. Yasir, Enhancement of Antibacterial Properties, Surface Morphology and In Vitro Bioactivity of Hydroxyapatite-Zinc Oxide Nanocomposite Coating by Electrophoretic Deposition Technique, Bioengineering, 10 (**2023**) 6, 693, doi:10.3390/bioengineering10060693

[15] G. Tripathi, V. H. Ho, H. I. Jung, B. T. Lee, Physico-mechanical and in-vivo evaluations of tri-layered alginate-gelatin/polycaprolactone-gelatin-β-TCP membranes for guided bone regeneration, J. Biomater. Sci. Polym. Ed., 34 (**2023**) 1, 18–34, doi:10.1080/09205063.2022.2106647

[16] H. Y. Liang, W. K. Lee, J. T. Hsu, J. Y. Shih, T. L. Ma, T. T. T. Vo, C. W. Lee, M. T. Cheng, I. T. Lee, Polycaprolactone in Bone Tissue Engineering: A Comprehensive Review of Innovations in Scaffold Fabrication and Surface Modifications, J. Funct. Biomater., 15 (**2024**) 9, 243, doi:10.3390/jfb15090243

[17] I. Lhotská, M. Háková, J. Erben, J. Chvojka, F. Švec, D. Šatínský, Stirred discs from polycaprolactone nanofibers highly doped with graphene for straightforward preconcentration of pollutants in environmental waters, Talanta, 266 (**2024**) 1, 124975, doi:10.1016/j.talanta.2023.124975

[18] P. S. Poh, D. W. Hutmacher, B. M. Holzapfel, A. K. Solanki, M. A. Woodruff, Data for accelerated degradation of calcium phosphate surface-coated polycaprolactone and polycaprolactone/bioactive glass composite scaffolds, Data Brief., 7 (**2016**), 923–926, doi:10.1016/j.dib.2016.01.023

[19] C. Yu, J. Chen, T. Wang, Y. Wang, X. Zhang, Z. Zhang, Y. Wang, T. Yu, T. Wu, GelMA hydrogels reinforced by PCL@GelMA nanofibers and bioactive glass induce bone regeneration in critical size cranial defects, J. Nanobiotechnology, 22 (**2024**) 1, 696, doi:10.1186/s12951-024-02980-w

[20] M. Janmohammadi, N. Doostmohammadi, M. Bahraminasab, M. S. Nourbakhsh, S. Arab, S. Asgharzade, A. Ghanbari, A. Satari, Evaluation of new bone formation in critical-sized rat calvarial defect using 3D printed polycaprolactone/tragacanth gum-bioactive glass composite scaffolds, Int. J. Biol. Macromol., 270 (**2024**) 1, 132361, doi:10.1016/j.ijbiomac.2024.132361

[21] G. Marchiori, D. Bellucci, A. Gambardella, M. Petretta, M. Berni, M. Boi, B. Grigolo, G. Giavaresi, N. Baldini, V. Cannillo, C. Cavallo, A Multidisciplinary Evaluation of Three-Dimensional Polycaprolactone Bioactive Glass Scaffolds for Bone Tissue Engineering Purposes, Materials, 17 (**2024**) 10, 2413, doi:10.3390/ma17102413